Design of a Compact 900 MHz Class-F Power Amplifier with Efficiency Improvement using Modified Harmonic Control Circuit

Rasoul Azadi[1], Saeed Roshani[2*], Arez Nosratpour[3], Mohammad Hazhir Mozaffari[4]
1- Department of Electrical Engineering, Sanandaj Branch, Islamic Azad University, Sanandaj, Iran.
Email: azadirasol1989@gmail.com
2- Department of Electrical Engineering, Kermanshah Branch, Islamic Azad University, Kermanshah, Iran.
Email: s_roshany@yahoo.com (Corresponding author)
3- Department of Electrical Engineering, Sanandaj Branch, Islamic Azad University, Sanandaj, Iran.
Email: a.nosratpour@iausdj.ac.ir
4- Department of Electrical Engineering, Sanandaj Branch, Islamic Azad University, Sanandaj, Iran.
Email: mh.mozaffari@iausdj.ac.ir

Received: 15 January 2023 Revised: 3 February 2023 Accepted: 25 March 2023

ABSTRACT:
A Harmonic Control Circuit (HCC) is one of the most important blocks in the Class-F power amplifiers, which should pass the even harmonics and suppress the odd harmonics. Long open stubs are usually used to suppress odd harmonics in the conventional Class-F power amplifiers, which resulted in the large size of the amplifiers. In this work, two Class-F amplifiers are designed, a simple amplifier with traditional HCC and proposed PA with a proposed HCC. The proposed HCC suppresses third, fifth and seventh harmonics and easily pass second, fourth and sixth harmonics. In the proposed amplifier with proposed HCC, the design parameters are improved compared to the simple Class-F with traditional HCC. The power added efficiency (PAE), drain efficiency (DE) and gain parameters are increased from 76%, 79% and 19.4 dB to 79.2%, 82.2% and 21.2 dB, respectively. The proposed PA is fabricated, measured and results show that the proposed PA correctly works at 0.9 GHz with 0.12 GHz bandwidth.

KEYWORDS: Class-F Power Amplifier, Harmonic Suppression, Harmonic Control Circuit (HCC), Power Amplifier (Pa).

1. INTRODUCTION

Nowadays, amplifiers are extensively applied in modern communication circuits and systems.

Power amplifiers are widely used in the communications systems and they are categorized into two major groups of current-mode and switching-mode amplifiers. Current-mode amplifiers, such as: class A, B, C and AB have higher linearity, but they suffer from low efficiency, which increases power consumption [1].

Switching-mode amplifiers, such as class F amplifiers are based on the harmonic terminations synthesized across the active device. Switched-mode amplifiers, such as: class E, D, G, H, S and etc. are performed by identifying the switching duty-cycle and/or the switching combination [2]. The class-F power amplifier uses the multiple harmonics resonators to control the harmonics to shape voltage and drain current waveforms, thereby shaping them to reduce the power dissipation by the transistor and thus to increase the efficiency of the power amplifier [3]. In an ideal class-F power amplifier the efficiency is 100% and is achieved by using an infinite number of harmonics to yield square and half-wave sinusoid waveform shapes at device drain for the voltage and current respectively. In real, several open/short stubs are used to control harmonics, which occupied large areas. In past decade, several methods are used to control harmonics in class-F amplifiers, which are described as follows.

In [4], a nonlinear transfer function is introduced for a Class-F PA and the drawback of the second harmonics is modified in this work.

In [5], a simple impedance matching network is presented to control harmonics in Class-F and Class-F-1 amplifiers with lumped components. Unfortunately, applied lumped components in this work restrict operating frequency. In [6] extended formulation for the voltage waveform in the Class-F PA and in [7] analysis for the current waveform in the Class-F^{-1} amplifier are

Paper type: Research paper
DOI: 10.30486/mjee.2023.1970148.0
How to cite this paper: R. Azadi, S. Roshani, A. Nosratpour and M. H. Mozaffari, **"Design of a Compact 900 MHz Class-F Power Amplifier with Efficiency Improvement using Modified Harmonic Control Circuit"**, Majlesi Journal of Electrical Engineering, Vol. 17, No. 2, pp. 133-143, 2023.

presented. With these formulations, high-efficiency amplifiers are designed. In [8], a CMRC cell is applied as a harmonic control block of the Class-F amplifier. This cell only suppresses 3rd harmonics and increases the efficiency of the PA. In [9], three-stage output matching network is used to have a multi-harmonic-controlled Class-F amplifier. With this method, efficiency of PA is increased. In [10], a band pass filter is integrated with a Class-F amplifier. The applied BPF works as a harmonic control circuit and suppresses 3rd harmonics, which resulted in a high-efficiency amplifier. In [11], a Class-F and a Class-F-1 amplifiers are designed and used to create a Doherty power amplifier (DPA). In this structure, Class-F PA is used as a peaking amplifier and inverse Class-F PA is used as a carrier amplifier. In this work, the linearity parameter of the applied amplifier is increased with Doherty structure. In [12], a Class-F and an inverse Class-F amplifiers are designed and used to create a continuous mode hybrid amplifier for 5G application. This structure presents a high-efficiency amplifier.

In [13], lumped components are used to create small size Class-F amplifier with high efficiency. In this design, capacitors are used to reduce the long conventional stubs, which are used in the HCC part of the Class-F amplifier. In this design, lumped elements components are used to create small composite lines. These compact composite lines are used as a new way to reduce the dimensions of the applied microstrip harmonic control circuit (HCC) structure and to reduce overall size of the class F amplifiers. In this design, at first, traditional class-F amplifier with traditional HCC is designed then modified PA with compact HCC is designed with composite lines.

Using this design, the efficiency is increased but applied of external components limits portaging frequency and it is not a desirable method. In [14], high-efficiency Class-F PA is presented with a harmonic termination technique (HTT). In this work, the bias lines of gate and drain are used in the HTNs to reduce the circuit size. In [15], a wide band Class-F^{-1} amplifier is designed. In this work, a low-pass filter is used as a matching network. Due to the wide operating band, the second harmonics has a wide band, which correctly suppressed with applied LPF. With this applied matching network the performance of designed PA is increased. A compact class-F power amplifier is presented in [16], and accomplished with new small HCC block, at 900 MHz frequency. The small size meandered microstrip resonant cell (MLCMRC), with simple structure is used as a harmonic control circuit (HCC).

In [17], a LPF is used as HCC in class-F amplifier structure. Applied LPF suppresses both odd and even harmonics and it seems that the harmonic control circuit does not work correctly in this design.

In [18], harmonic tuning mechanism is used to design 10 wats class-F amplifier for 5G mobile applications. The HCC block in this design controls second and third harmonics and improves the performance of the PA.

In [3], a compact class-F PA is designed at 900 MHz frequency, which in this structure meandered line compact microstrip resonant cell (MLCMRC), is used as a harmonic control circuit (HCC). In this structure, the applied PA is integrated with simple MLCMRC, and huge conventional matching lines are removed, which leads to size reduction and harmonics suppression together. The applied MLCMRC resulted in the 36% size reduction, compared to the same PA without MLCMRC.

In [19], a class-F amplifier for GSM applications is designed at 1.8 GHz, which in this structure symmetrical meandered lines compact microstrip resonant cell (SMLCMRC), is applied as a harmonics control circuit (HCC), which resulted in size reduction in the PA. This applied structure, which is used as HCC resulted in performance improvement of Class-F amplifier.

In [20], a high-efficiency class-F PA with a harmonic control circuit is designed. The HCC is designed by using microstrip branch lines to achieve a short-circuit state for the second harmonic. The double spiral defected ground units are loaded on the ground of the microstrip line of the drain bias circuit to produce a low-pass filtering and stopband suppression effect outside the passband, so as to suppress the third harmonic. This structure resulted in efficiency improvement of the designed Class-F PA.

In all of the mentioned works only one or two odd harmonics are suppressed in Class-F PAs and only one or two even harmonics are suppressed in Class-F^{-1} PAs. In the designed amplifier, three odd harmonics are eliminated with the proposed HCC network, which resulted in a high-efficacy power amplifier. Moreover in this paper two class-F amplifiers are designed and simulated (traditional PA and proposed PA). The sufficient equations and analysis are provided for designed PA. At last, proposed design is fabricated and measured. The measured results validated the simulations and provided theoretical analysis.

2. THE RESONATOR DESIGN

In the proposed power amplifier structure, a resonator is used as a HCC block. This block must eliminate odd harmonics and pass even harmonics. The schematic diagram of the primitive resonator is depicted in Fig.1.

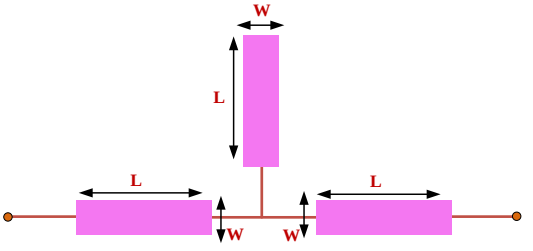

Fig. 1. The primitive resonator structure.

The primitive resonator consists of three same stubs. The LC-equivalent circuit is used to achieve the best dimensions and performance. The LC-equivalent circuit of the simple microstrip line is demonstrated in Fig. 2.

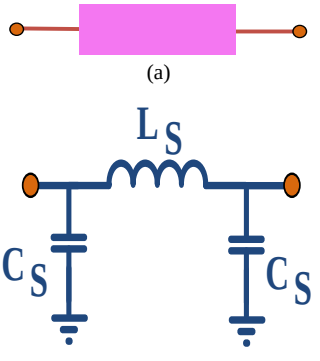

Fig. 2. Structure of the (a) simple microstrip line and (b) its LC- model.

Each stub can be equated with two capacitors (Cs) and an inductance (Ls). The values of capacitors and an inductor are obtained from (1) and (2).

$$Ls = \frac{1}{2\pi f} \times Z_s \times Sin\left(\frac{2\pi L}{\lambda g}\right) \quad (1)$$

$$s = \frac{1}{2\pi f} \times \frac{1}{Z_s} \times Tang\left(\frac{\pi L}{\lambda g}\right) \quad (2)$$

The LC model of the primitive resonator is displayed in Fig. 3(a) and the scattering parameters of this circuit are depicted in Fig.3(b).

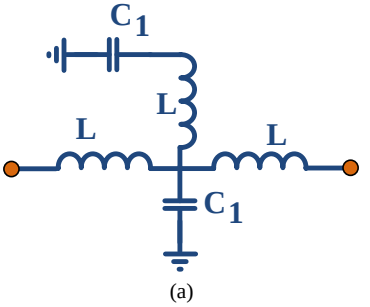

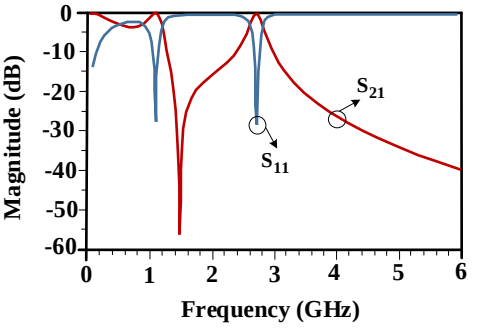

Fig. 3. The primitive resonator (a). LC equivalent circuit, (b) scattering parameters.

The structure of the Primitive resonator and its frequency responses are depicted in Fig. 4(a) and Fig. 4(b), respectively. This resonator contains three open-ended stubs, with different lengths, which create three transmission zeros. This structure is suitable to use as HCC in class-F amplifiers but it consumes large size.

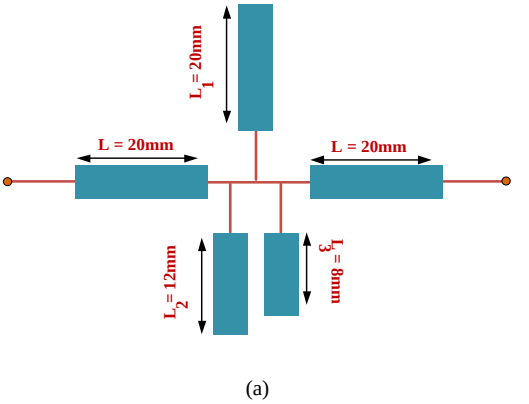

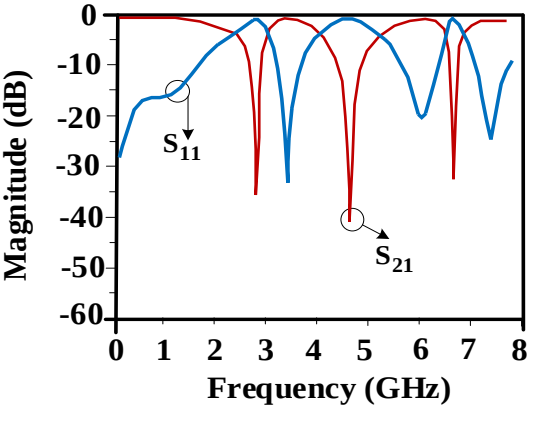

Fig. 4. Primitive resonator. (a) design (b) frequency response.

2.1. Analysis of the Resonator

In the HCC design, the HCC should suppress odd harmonics and pass even harmonics. If the Yodd or Yeven are zero, the transmission zero and pole of the system can be calculated. The equation of Yeven is calculated in (3) and diagram of (3) is displayed in Fig. 5, all impedance will be assumed 50 ohms.

$$Yeven = -50I\text{Cot}[\text{t1}] \quad (3)$$

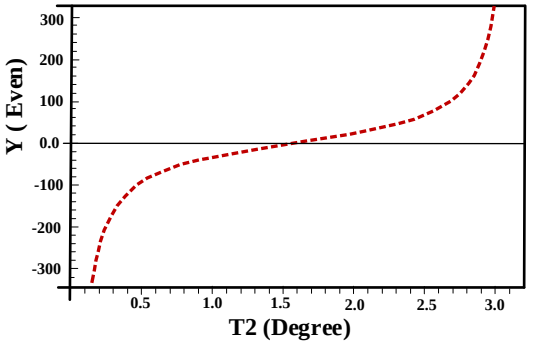

Fig. 5. Diagram of the Yeven transmission line.

Based on the Fig. 5, the Yeven is zero at 1.5 which is equal to 90 degrees. So the length of line at 1Ghz with substrate of RT-5880 and H=20 mil is about 40 mm which can divided to the two or four parts, like the structure, depicted in Fig.6. This block must eliminate odd harmonics and pass even harmonics.

The schematic diagram of the even-mode and odd-mode are exhibited in Fig.7a and Fig.7b, respectively.

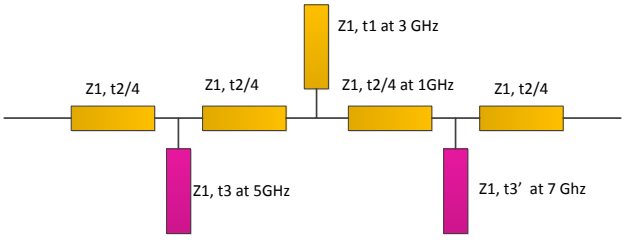

Fig. 6. The structure of the principle resonator.

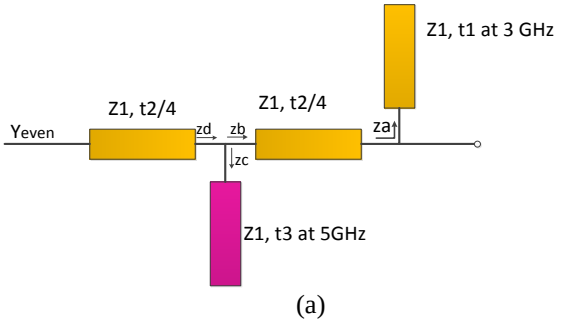

(a)

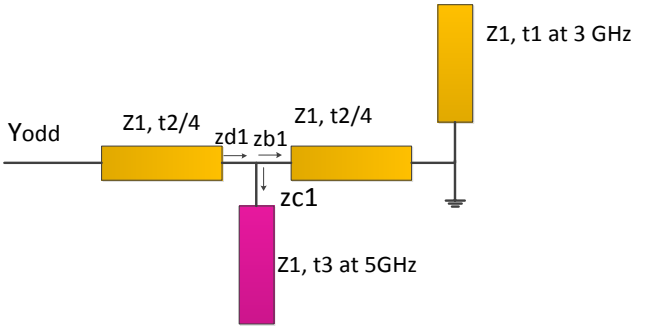

(b)

Fig. 7. The main resonator (a) even-mode and (b) odd-mode.

The equations of Yeven are summarized from (4) to (8).

$$\text{za} = -izlCot[t1] \quad (4)$$

$$\text{zb} = \frac{\text{izl}(\text{Cot}[\text{t1}]-\text{Tan}[\text{t2}])}{1+\text{Cot}[\text{t1}]\text{Tan}[\text{t2}]} \quad (5)$$

$$\text{zc} = -\text{izlCot}[\text{t3}] \quad (6)$$

Zc and Zb are parallel and equaled in Zd and (7).

$$zd = \frac{izlCot[t3](Cot[t1]-Tan[t2])}{Cot[t1]+Cot[t3]-Tan[t2]+Cot[t1]Cot[t3]Tan[t2]} \quad (7)$$

$$Yeven = -\frac{i(\text{Cot}[\text{t1}]+\text{Cot}[\text{t3}]+(-1+2\text{Cot}[\text{t1}]\text{Cot}[\text{t3}])\text{Tan}[\text{t2}]-\text{Cot}[\text{t3}]\text{Tan}[\text{t2}]^2)}{\text{zl}((2\text{Cot}[\text{t3}]-\text{Tan}[\text{t2}])\text{Tan}[\text{t2}]+\text{Cot}[\text{t1}](\text{Tan}[\text{t2}]+\text{Cot}[\text{t3}](-1+\text{Tan}[\text{t2}]^2)))} \quad (8)$$

Based on Fig. 5 t2 was 90˚ but it is divided to four parts (or two part) so it is 22.5˚ (or 45˚) also t3 will be calculated by Yodd from (9) - (12).

$$Zb1 = izlTan[t2] \quad (9)$$

$$Zc1 = izlCot[t3] \quad (10)$$

Zc1 and Zb1 are parallel and equaled in Zd1 and (11).

$$Zd1 = \frac{i\text{zlCot}[\text{t3}]\text{Tan}[\text{t2}]}{\text{Cot}[\text{t3}]-\text{Tan}[\text{t2}]} \quad (11)$$

$$Yodd = \frac{i(-Cot[t3]+Tan[t2]+Cot[t3]Tan[t2]^2)}{zl(-2Cot[t3]Tan[t2]+Tan[t2]^2)} \quad (12)$$

The response of Yodd and Yeven are depicted in Fig.8a and Fig.8b.

Both of them approximately at 1.5 or 90 degrees are zero so the left pink open stub line (t3) will be 12 mm which produces transmission zero at 4.5 GHz and the left one (t3') is 8 mm which produces transmission zero at 6.3 GHz. And t1 is 20 because it is adjusted to produce transmission zero at 2.7 GHz.

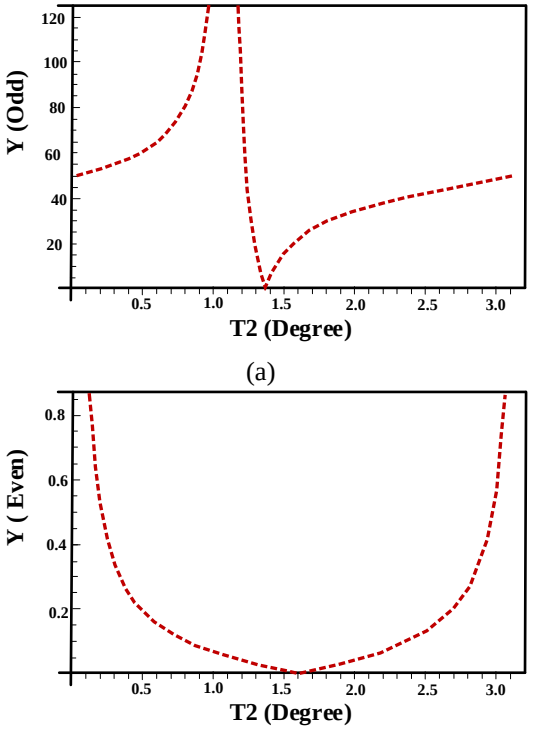

Fig. 8. The response of (a) odd-mode (b) even-mode.

The main resonator based on the calculated dimension is exhibited in Fig. 9.

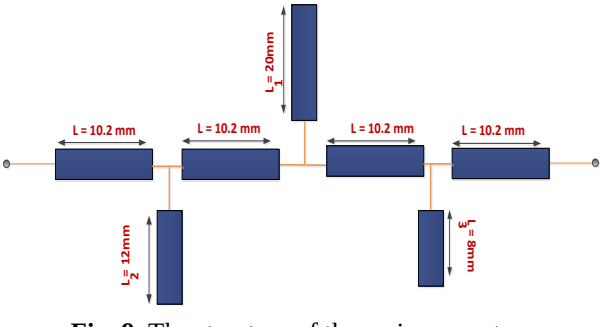

Fig. 9. The structure of the main resonator.

This design with one open stub creates a transmission zero (TZ). To have extra TZs, more open-ended stubs are used to shape the main resonator with new dimensions. The main resonator is designed and demonstrated in Fig. 4a and its S-parameters are shown in Fig. 4b. The scattering parameters show that the main resonator creates three TZs at 2.7 GHz, 4.5 GHz and 6.3 GHz. The length of these three open-ended lines are obtained as 20, 12 and 8 mm. The main resonator is designed to be used as a HCC of the Class-F PA. So, if the main frequency of PA is 0.9 GHz, therefore the main resonator is suppressed third, fifth, seventh harmonics of the amplifier. The length and width of applied stubs in part 2, are 60.5 mm and 2.7mm. Also to calculated exact dimensions, even and odd mods are used.

The main resonator correctly suppresses three unwanted harmonics but occupied large areas to reduce the occupied area, modified T-shaped resonator and meander structure are used instead of simple long lines in the main resonator. The structure of the designed resonator and its S-parameters illustrated are shown in Fig. 10(a) and 10(b).

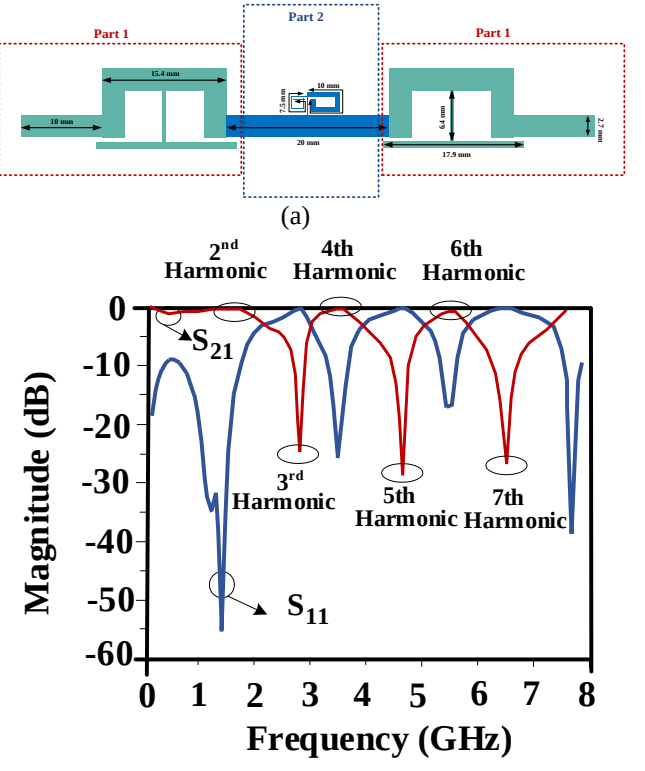

Fig. 10. The proposed resonator (a) Structure. (b) frequency response.

3. CLASS-F AMPLIFIER DESIGN

In this paper, two Class-F power amplifiers are designed. The primitive one with simple HCC and proposed PA with the designed HCC, which results show the performance improvement of the proposed PA.

The primitive Class F PA

The primitive and proposed Class-F amplifiers are designed using ATF-34143 transistor on the Rogers RT/duroid 5880 substrate, which has a very low dielectric loss with 2.2 dielectric constant and 0.508 mm thickness.

The structure of the primitive Class F PA is shown in Fig. 11(a). In this structure, only simple microstrip stubs are used. The S-parameters for the primitive amplifier are depicted in Fig. 11(b). The primitive amplifier has a more than 20 dB small-signal gain at 900 MHz. The current and voltage curves of the primitive PA are

depicted in Fig. 11(c). The voltage curve is approximately half rectangular shaped and the current curve is approximately half-sine, which shows the correct performance of the primitive PA. Fig. 11(d) shows a small gain variation of the primitive Class-F PA for different values of L_1.

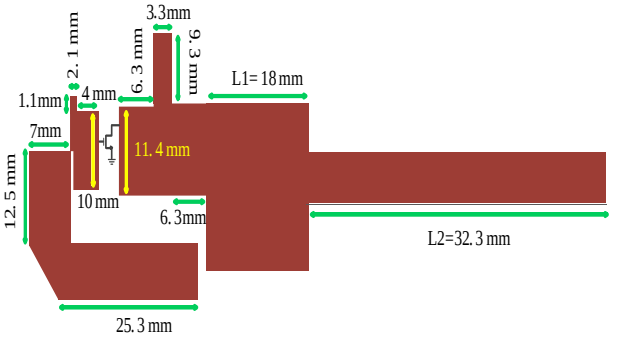

(a)

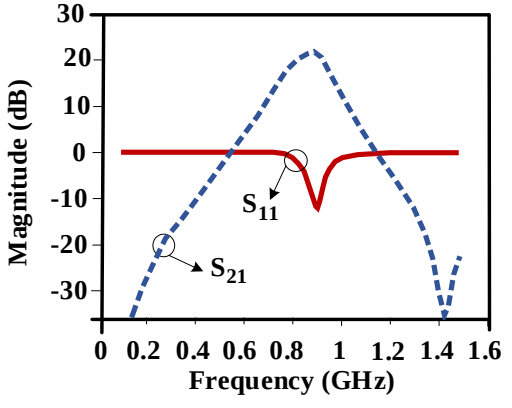

(b)

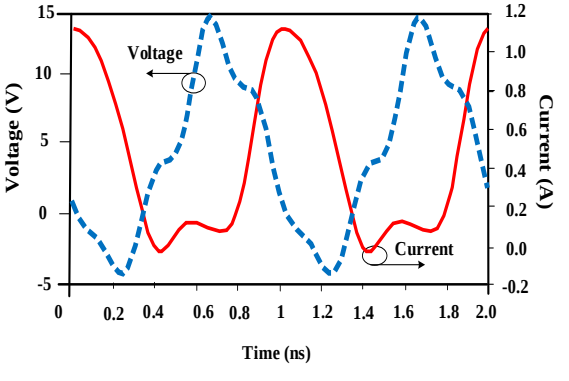

(c)

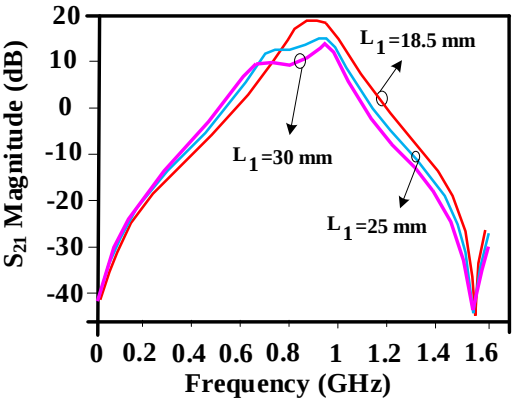

(d)

Fig. 11. The(a) structure of the primitive Class-F power amplifier (b) scattering parameters (c) voltage and current curves (d) effect of L_1 on the S_{21}.

The drain efficiency (DE), power added efficiency (PAE), and gain parameters of the primitive amplifier are displayed in Fig. 12. The DE, PAE and large-signal gain values at 900MHz are 79%, 76% and 19.4 dB, respectively.

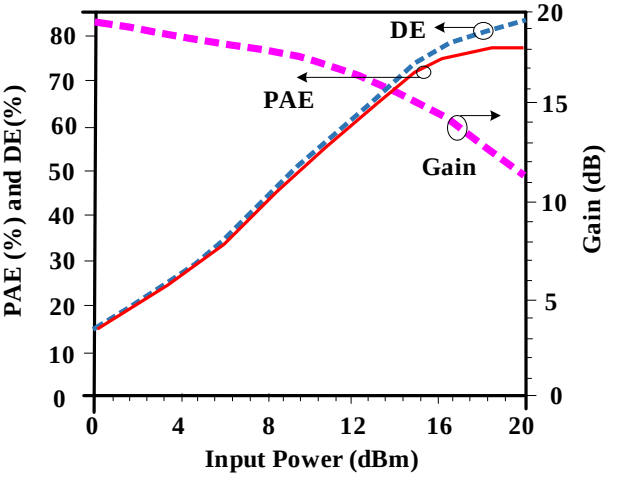

Fig. 12. The PAE, DE and gain of the primitive amplifier at 900 MHz.

3.1. The Proposed Class-F PA

The primitive amplifier has an acceptable performance but using this device does not result in superior results. The output matching network in primitive amplifier is consist of the simple two-section block (L_1 and L_2). This block is very large and only suppresses 3rd harmonic. To improve the PA performance, the proposed resonator is used instead of this large block. The proposed resonator has a smaller size and reduces 3rd, 5th and 7th harmonics, which resulted in performance improvement.

The layout of the designed amplifier is depicted in Fig. 13(a) and Fig. 13 (b) illustrates the S_{21} parameter of the designed PA at the 0.9 GHz operating frequency with about 0.12 GHz bandwidth. This parameter is more than 23 dB. The current and voltage curves of the designed PA are depicted in Fig. 13(c). The voltage curve is half rectangular shaped and the current curve is a half-sine.

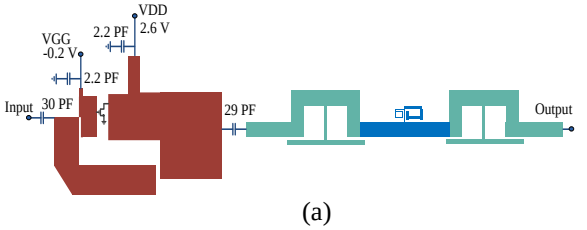

(a)

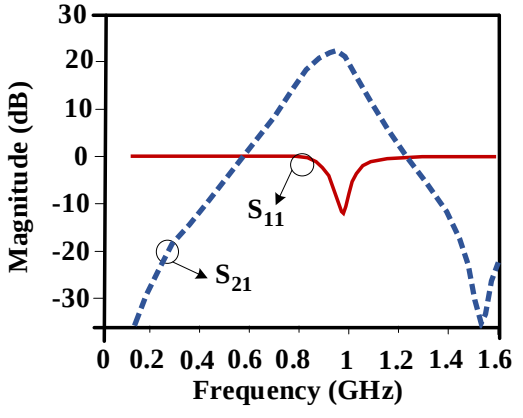

(b)

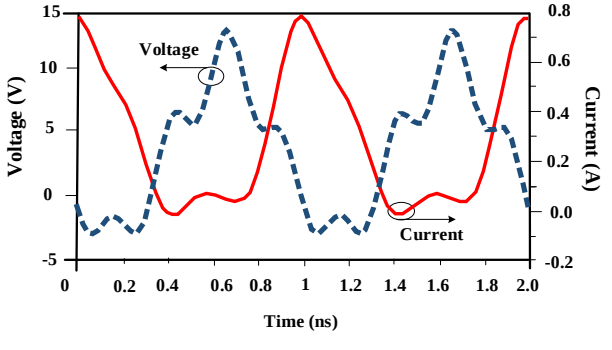

(c)

Fig. 13. The (a) Layout, (b) scattering parameters, (c) voltage and current curves of the designed Class-F power amplifier.

The proposed resonator correctly, passes second, fourth, and sixth (even) harmonics and suppresses third, fifth and seventh (odd) harmonics, which increase the performance of the designed amplifier. The PAE, DE and gain parameters of the proposed amplifier with designed resonator and simple Class-F PA without resonator are compared in Fig. 14. The PAE, DE and gain values for the simple PA are 76%, 79% and 19.4 dB, respectively and these parameters for the proposed PA are 79.2%, 82.2% and 21.2 dB, respectively. A performance comparison between amplifier with applied novel resonator and simple Class-F PA are listed in Table 1.

Table 1. A comparison between the proposed Class-F amplifier with resonator and simple one.

Par.	PAE	DE	Gain
Simple Class-F PA without the resonator	76	79	19.4
Proposed Class-F PA with the resonator	79	82.2	21.2

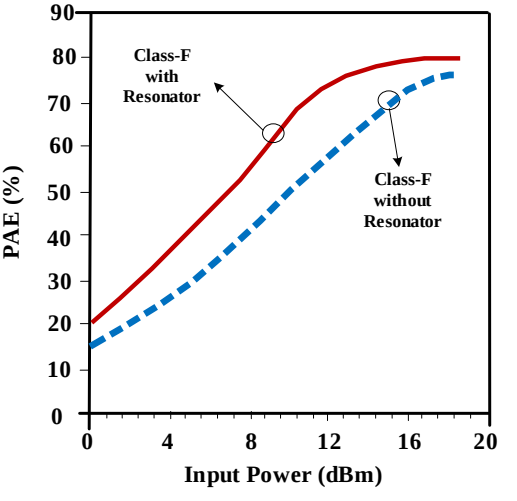

(a)

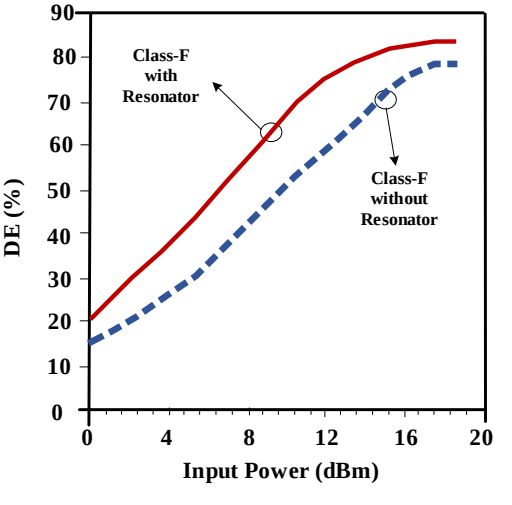

(b)

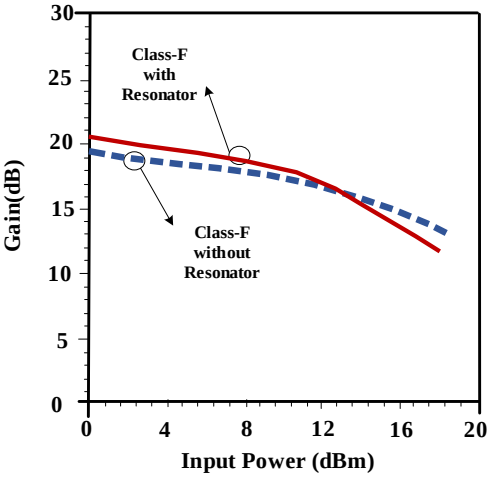

(c)

Fig. 14. The (a) PAE, (b) DE and (c) gain of the proposed PA.

4. MEASUREMENT RESULTS

The designed amplifier is simulated using Agilent ADS software. The DC bias point of the applied ATF-34143 transistor is defined as Vdd = 2.6 V and Vgg = -0.2V. The designed PA is fabricated on the Rogers substrate with the mentioned specifications, as illustrated in Fig. 15.

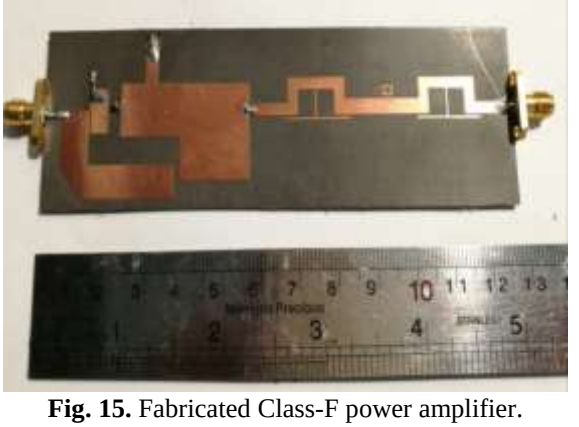

Fig. 15. Fabricated Class-F power amplifier.

The proposed PA is simulated and measured. The simulation and measurement results are depicted in Fig. 16(a) and the measured results photo is shown in Fig.16 (b). The designed amplifier correctly works at 0.9 GHz with 120 MHz bandwidth. The performance comparison of the designed PA with similar works is shown in Table 2. As results show, the proposed PA has good performances.

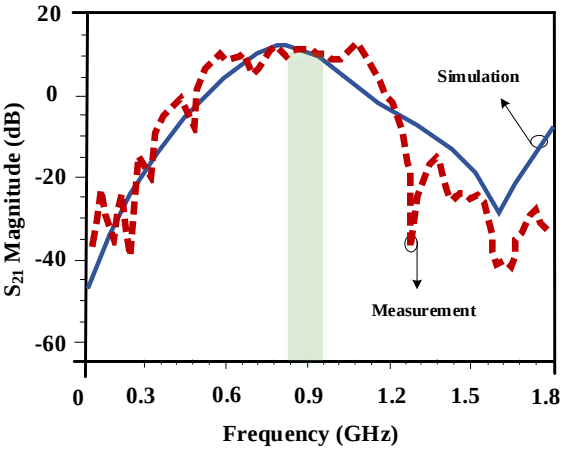

(a)

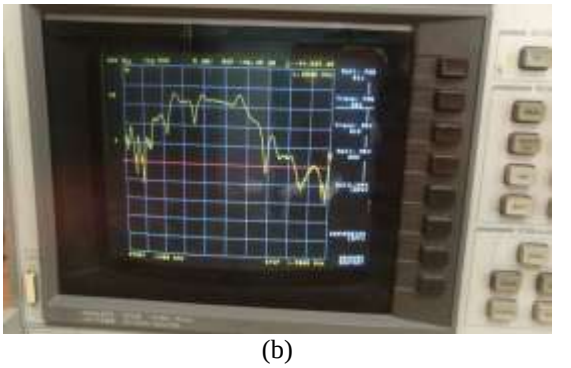

(b)

Fig. 16. The measurement results of the fabricated amplifier. (a) simulation and measurement. (b) measured results photo.

The measured PAE, DE and gain parameters of the fabricated PAE versus output power are depicted in Fig. 17.

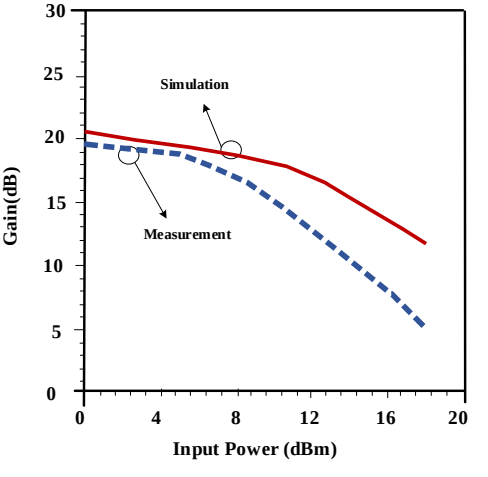

(a)

Table 2. A performance comparison between the designed amplifier and some similar reported works.

Refs.	Freq. (GHz)	Operation Classes	DC Voltage of Drain (V)	Max. PAE (%)	DE (%)	Max. Gain (dB)
[3]	0.9	F	-	74	76	18.5
[5]	0.3	F/F^{-1}	28	-	81/79	-
[9]	3.1	F	28	82	85	15
[10]	2.4	F	28	70.9	75/5	18.2
[11]	2.4	F	28	-	82.2	7
[13]	2.4	F	3	80	86	11.5
[15]	1.35 - 2.5	F^{-1}	-	-	68-82	15.2-17
[16]	1.75	F	-	74	-	18.3
[17]	3.6	F	28	59.6	64.7	11.2
[19]	2.6	F^{-1}	48	-	-	17.8
[21]	0.5-2.3	F	28	52.7-80.7	60-81	11.7-25.3
[22]	2.2-2.8	F-1	28	65	65.9	18
[23]	2.6	G/F-1	28	75	82	12
[24]	0.6 - 1.15	F/F^{-1}	27	-	77.5	-
[25]	2	F	42.5	85	91	15.8
[26]	1.88	F	28	70.7	75.8	18.3
[27]	2.4	F	3	74	-	10
[28]	2.4	F^{-1}	32	-	49	-
[29]	0.9	F	5	74	75	18.5
Proposed work	0.9	F	2.6	79	82.2	21.2

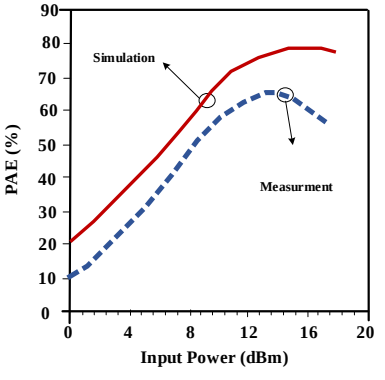

(b)

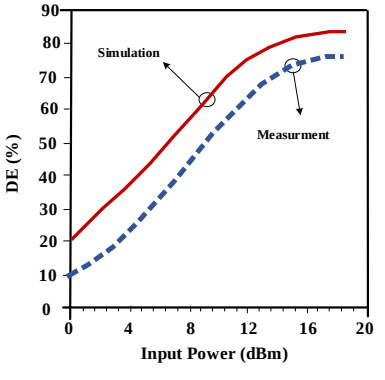

(c)

Fig. 17. The simulated and measured (a) gain, (b) PAE and (c) DE curves of the fabricated PA versus input power.

The simulated and measured results of the output power versus input power for the fabricated class-F amplifier are shown in Fig. 18. The 1 dB compression point (P1dB) for the proposed class-F amplifier is 31 dBm at 12 dBm input power and for the proposed class-F PA, showing that the proposed PA has linear preference below this point.

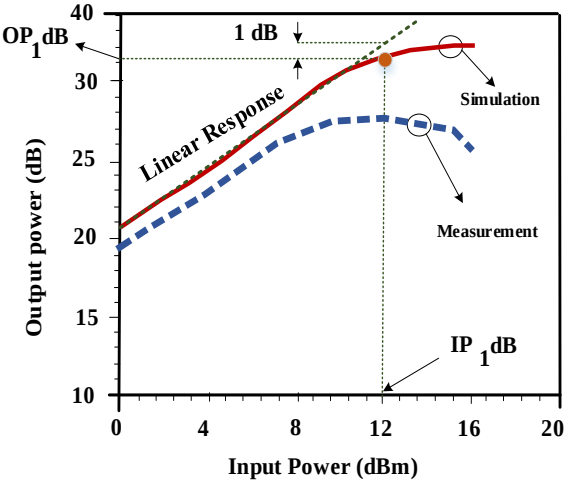

Fig. 18. The simulated and measured output power curves of the fabricated PA versus input power.

5. CONCLUSION

In this paper, a new resonator is designed to control harmonics in the Class-F PA. The proposed resonator suppresses 3rd, 5th and 7th harmonics and passes 2nd, 4th and 6th harmonics, which resulted in gain, PAE and DE increment in the proposed Class-F power amplifier. The gain, PAE and DE parameters of the proposed PA are 21.2 dB, 79% and 82.2%. The operating frequency and bandwidth of the proposed amplifier are 0.9 GHz and 0.12 GHz, respectively. The proposed device with these features is suitable for the 5G application.

REFERENCES

[1] P. Colantonio, F. Giannini, E. Limiti, **"High Efficiency RF and Microwave Solid State Power Amplifiers,"** *John Wiley & Sons*, 2009.

[2] F.H. Raab, **"An introduction to class-F power amplifiers,"** *RF Design* 19 (5) , pp. 79–84, 1996.

[3] Sa. Roshani, and So. Roshani, **"Design of a high efficiency class-F power amplifier with large signal and small signal measurements,"** *Measurement*, Vol. 149, pp.1069-1091, 2020.

[4] E. Aggrawal, K. Rawat, and P. Roblin, **"Investigating continuous class-F power amplifier using nonlinear embedding model, "** *IEEE Microwave and Wireless Components Letters*, Vol. 27, pp.593-595, 2017.

[5] R.A. Beltran, **"Class-F and inverse class-F power Amplifier loading networks design based upon transmission zeros,"** presented at *the IEEE MTT-S International Microwave Symposium*, pp. 1-4, Tampa, FL, USA, 2014.

[6] V. Carrubba, A. L. Clarke, M. Akmal, J. Lees, J. Benedikt, P.J. Tasker, and S.C. Cripps, **"On the extension of the continuous class-F mode power amplifier, "** *IEEE Transactions on Microwave Theory and Techniques*, Vol. 59, pp.1294-1303, 2011.

[7] V. Carrubba, M. Akmal, R. Quay, J. Lees, J. Benedikt, S.C. Cripps, and P.J Tasker**, "The continuous inverse class-F mode with resistive second-harmonic impedance, "** *IEEE Transactions on Microwave Theory and Techniques*, Vol. 60, pp.1928-1936, 2012.

[8] S. Chen, Q. Xue, **"A class-F power amplifier with CMRC, "** *IEEE Microwave and Wireless components letters*, Vol. 21, pp. 31-33, 2010.

[9] K. Chen, and D. Peroulis, **"A 3.1-GHz class-F power amplifier with 82% power-added-efficiency, "** *IEEE Microwave and Wireless Components Letters*, Vol. 23, pp.436-438, 2013.

[10] Q.Y. Guo, X.Y. Zhang, J.X. Xu, Y.C. Li, and Q. Xue, **"Bandpass class-F power amplifier based on multifunction hybrid cavity microstrip filter, "** *IEEE Transactions on Circuits and Systems II: Express Briefs*, Vol. 64, pp.742-746, 2016.

[11] J. Kim, **"Highly efficient asymmetric class F^{-1}/F GaN Doherty amplifier, "** *IEEE Transactions on Microwave Theory and Techniques*, Vol. 66, pp.4070-4077, 2018.

[12] T.W. Li, and H. Wang, **"A continuous-mode 23.5-41GHz hybrid class-F/F^{-1} power amplifier with 46% peak PAE for 5G massive MIMO applications,"** presented at *the IEEE Radio Frequency Integrated Circuits Symposium (RFIC).* pp. 220-230, Philadelphia, USA. 2018.

[13] A. Pirasteh, Sa. Roshani, and So. Roshani, **"Design of a miniaturized class F power amplifier using capacitor loaded transmission lines,"** *Frequenz*, Vol. 74, pp.145-152, 2020.

[14] G. Nikandish, E. Babakrpur, and A. Medi, **"A harmonic termination technique for single-and multi-band high-efficiency class-F MMIC power amplifiers,"** *IEEE Transactions on Microwave Theory and Techniques*, Vol. 62, pp. 1212-1220, 2014.

[15] M. Yang, J. Xia, Y. Guo, and A. Zhu, A. **"Highly efficient broadband continuous inverse class-F power amplifier design using modified elliptic low-pass filtering matching network,"** *IEEE Transactions on Microwave Theory and Techniques*, Vol. 64, pp.1515-1525, 2016.

[16] S.Y. Zheng, Z.W. Liu, X.Y. Zhang, X.Y. Zhou, and W.S. Chan, **"Design of ultra-wide band high-efficiency extended continuous class-F power amplifier,"** *IEEE Transactions on Industrial Electronics, Vol.* 65, pp. 4661-4669, 2017.

[17] N. Poluri, and M.M. De Souza, **"High-Efficiency Modes Contiguous with Class B/J and Continuous Class F^{-1} Amplifiers,"** *IEEE Microwave and Wireless Components Letters*, Vol. 29, pp. 137-139, 2019.

[18] T. Sharma, ER. Srinidhi, R. Darraji, DG. Holme, J. Staudinger, JK. Jones, F.M. Ghannouchi, **"High-efficiency input and output harmonically engineered power amplifiers,"** *IEEE Transactions on Microwave Theory and Techniques*. Vol. 66, pp.1002-14, 2017.

[19] A. Pirasteh, Sa. Roshani, and So. Roshani, **"A modified class-F power amplifier with miniaturized harmonic control circuit,"** *AEU-International Journal of Electronics and Communications*, Vol. 97, pp.202-209, 2018.

[20] W. Huang, J. Liu. **"High-efficiency class-F power amplifier based on double spiral defected ground structure,"** *International Journal of Electronics.* 2023.

[21] S. Abbasian, T. Johnson, **"Power efficiency characteristics of class-F and inverse class-F synchronous rectifiers,"** *IEEE Transactions on Microwave Theory and Techniques*, Vol. 64, pp. 4740-4751, 2016.

[22] D. Schmelzer, and S.I. Long, **"A GaN HEMT Class F Amplifier at 2 GHz with 80% PAE,"** *IEEE Journal of Solid-State Circuits, Vol.* 42, pp.2130-2136, 2007.

[23] J.X. Xu, X.Y. Zhang, and X.Q. Song, **"High-efficiency filter-integrated class-F power amplifier based on dielectric resonator,"** *IEEE Microwave and wireless components Letters*, Vol. 27, pp.827-829, 2017.

[24] S. Chen, Q. Xue, **"A class-F power amplifier with CMRC,"** *IEEE Microwave and Wireless*

components letters, Vol. 21, pp. 31-33, 2010.

[25] H.C. Chang, Y. Hahn, P. Roblin, and T.W. Barton, **"New mixed-mode design methodology for high-efficiency out phasing chireix amplifiers,"** *IEEE Transactions on Circuits and Systems I,* Vol. 66, pp.1594-1607, 2018.

[26] T. Sharma, J. Roberts, D.G. Holmes, R. Darraji, J.K. Jones, and F.M. Ghannouchi, **"On the double-inflection characteristic of the continuous-wave AM/AM in class-F^{-1} power amplifiers,"** *IEEE Microwave and Wireless Components Letters*, Vol. 28, pp.1131-1133, 2018.

[27] J. Kim, **"2.4 GHz Class-F-1 GaN Doherty Amplifier With Efficiency Enhancement Technique,"** *IEEE Microwave and Wireless Components Letters,* Vol. 28, pp.34-36, 2017.

[28] M. Parnianchi,**"High-efficiency class-F Power amplifier with a new design of input matching network,"** *International Journal of Circuits, Systems and Signal Processing,* Vol. 16, pp.865-873, 2022.

[29] M. Sajedin, M., I. T. Elfergani, J. Rodriguez, M. Violas, A.S. Asharaa, R.A. Abd-Alhameed, M. Fernandez-Barciela, and A.M. Abdulkhaleq, "**Multi-Resonant Class-F Power Amplifier Design for 5G Cellular Networks,"** *RADIOENGINEERING,* 2021.